

# A COMPRESSIBILITY CORRECTIONS OF THE PRESSURE STRAIN LINEAR PART MODELS

by

*Hechmi KHLIFI*

Carthage University, Bizerte Preparatory Engineering Institute, Zarzouna-7021 Bizerte, Tunisia.

E-mail: [khlfihachmi@yahoo.fr](mailto:khlfihachmi@yahoo.fr)

*The main focus of this paper is the analysis of the compressibility effects and the validation of some recent Reynolds stress models for computing compressible turbulent flows. The pressure strain correlation is one of the several terms appearing in the Reynolds stress equation which directly reflect the compressibility effects on the turbulence. For this reason, a special attention is paid to the modeling of this term in order to account for compressibility effects at high-speed. The models developed by Speziale Sarkar and Gatski (SSG) and Fu, Launder and Tselepidakis (FLT) for the pressure strain correlation are examined to be extended to compressible turbulent flows. A compressibility corrections of these models using the turbulent Mach number are proposed. The calculations have been performed for the compressible homogeneous shear flow and the turbulent plate mixing layers. The comparison of the proposed compressibility modifications of the SSG and FLT models with its universal version shows some important ameliorations in results for the majority characteristic parameter of the structural compressibility effects. It's found that the predicted results from the modified SSG and FLT models are in reasonable agreement with the accepted data.*

Key words: *turbulence, compressible, pressure-strain, linear models of turbulence, homogeneous, mixing layer.*

## 1. Introduction

In the recent years, the research in the field of compressible turbulence has received considerable attention. These years marked by an increase of numerical[1,2,3,4,5,6], experimental[7,8] and modeling works allowed a better understanding of the compressibility phenomena. The reason behind motivation is that the advance in the compressible turbulence area is found to be essential for the development in designing a new generation of the supersonic aircraft and the high speed combustion. Many studies carried out last decade have shown that the compressibility has important effects on turbulence flows. One of the well known of these effects is the reduction of the turbulent kinetic energy redistribution phenomenon. Extensive studies have been conducted especially in the case of the compressible homogeneous shear flow. In this context, the DNS results led by Simone et al.[1] and by Sarkar[6] are selected as basic documents to understand some physical discrepancies of the compressibility effects on homogeneous turbulent shear flows. The analysis of these DNS results suggests that compressibility effects are related to extra-parameters : the turbulent Mach number ,  $M_t (M_t = \sqrt{2K} / \bar{a})$ , where  $\bar{a}$  is the mean speed of sound) and the gradient Mach number which is defined by :  $M_g = S\ell / \bar{a}$  , where

$S = (\tilde{U}_{i,j} \tilde{U}_{j,i})^{0.5}$  and  $\ell$  an integral length scale. The authors[1,3,6] have found out a notable decrease of the growth rate of the turbulent kinetic energy when the compressibility increases. According to the DNS results of Vreman et al.[4] and Pantano and Sarkar[5], Foysi et al.[2] and the experimental data of Goebel et al.[7], the compressibility strongly reduces the growth rate of turbulence mixing layers thickness with increasing convective Mach number  $M_C$ , this number is defined by [7]  $M_C = (\tilde{U}_1 - \tilde{U}_2)/(a_1 + a_2)$ . The subscript 1 denotes the value of the upper stream while the subscript 2 denotes the value of the lower stream. So the turbulence modeling is essential for predicting compressibility effects in agreement with numerical and experimental data. According to the DNS results of Sarkar[6] and Simone et al.[1], the changes of the turbulence structures are principally due to the structural compressibility effects. The authors suggest that this discrepancy is found in the role of the pressure. Thus, at high Mach number, the structural compressibility effects cause reduction of pressure strain correlation which leads to significant changes in turbulence structure as it is observed in the dramatic changes in magnitude of the Reynolds stress anisotropy components[1,3,6]. The DNS results [4,5] and the experiences[7,8] reached similar conclusions concerning the role of the pressure in the developed compressible plane mixing layers. As a consequence, in several studies[2,3,9,10], the pressure strain modeling has been considered as an important attractive research in the second order closure for the compressible turbulence flows.

An extension of the SSG[11] and FLT[12] incompressible models on compressible turbulent flows is the major aim of the present work. From this extension, two several models of Adumitroaie et al. [13] and Hung et al. [14] are selected to be used making the linear terms of these model [11,12] in dependence with the turbulent Mach number  $M_t$ . The ability of the different proposed compressibility corrections of the SSG and FLT models to predict compressible homogeneous shear flow and compressible mixing layers is examined by considering different initial conditions.

## 2. Governing equations

In general, compressible flow is described by the continuity, Navier –Stokes energy and state equations. They can be written as follow for continuity, momentum and energy conservation equations :

Continuity equation

$$\frac{\partial}{\partial t} \rho + \frac{\partial}{\partial x_i} \rho u_i = 0 \quad (1)$$

Momentum equation

$$\frac{\partial}{\partial t} \rho u_i + \frac{\partial}{\partial x_j} \rho u_i u_j = \frac{\partial}{\partial x_j} \sigma_{ij} \quad (2)$$

Specific internal energy equation

$$\frac{\partial}{\partial t} \rho e + \frac{\partial}{\partial x_j} \rho e u_j = \frac{\partial}{\partial x_j} \sigma_{ij} u_i - \frac{\partial}{\partial x_j} (\kappa T_{,j}) \quad (3)$$

State equation

$$p = \rho RT \quad (4)$$

where  $e = c_v T$ ,  $\sigma_{ij} = -p\delta_{ij} + \tau_{ij}$  and  $\tau_{ij} = 2\mu(u_{i,j} + u_{j,i})$ .

For compressible turbulent flow, it is well known that the basic equations of the mean quantities used in describing turbulence closure schemes are essentially those using the density weighting technique which is referred to as the Favre averages. One can remarks that the time-averaged resulting equations are formally similar to those governed incompressible turbulent flows. Obviously, this technique gives reason to extension of the incompressible turbulent models to study compressible turbulent flows. This is one of the essential advantages provided by the density weighting technique for modeling compressible turbulence. For this study, the Favre averaged continuity, momentum and specific internal energy equations are respectively written as follows :

$$\frac{\partial}{\partial t} \bar{\rho} + \frac{\partial}{\partial x_i} (\bar{\rho} \tilde{U}_i) = 0 \quad (5)$$

$$\frac{\partial}{\partial t} (\bar{\rho} \tilde{U}_i) + \frac{\partial}{\partial x_i} (\bar{\rho} \tilde{U}_i \tilde{U}_j) = \frac{\partial}{\partial x_j} (\bar{\sigma}_{ij} + \bar{\tau}_{ij}'' - \frac{\partial}{\partial x_j} \overline{\rho u_i'' u_j''}) \quad (6)$$

$$\frac{\partial}{\partial t} \bar{\rho} \tilde{e} + \frac{\partial}{\partial x_j} \bar{\rho} \tilde{e} \tilde{U}_j = -\bar{\varphi}_e + \bar{\pi}_d - \frac{\partial}{\partial x_j} \overline{c_v \rho u_j'' T''} \quad (7)$$

where:  $\bar{\varphi}_e = \bar{p} \frac{\partial}{\partial x_i} (\tilde{U}_i + \bar{u}_i'') + \frac{\partial}{\partial x_i} (\kappa \frac{\partial}{\partial x_i} T) + \overline{\tau_{ij} u_{i,j}}$ ,  $\bar{\tau}_{ij} = 2\mu \tilde{S}_{ij} - \frac{2}{3} \bar{\mu} \tilde{U}_{k,k} \delta_{ij}$  and  $\bar{\pi}_d = \overline{p' u_{i,i}'}$

The Favre averaged Reynolds stress  $R_{ij} = \overline{\rho u_i'' u_j''} / \bar{\rho}$  are described by equation, namely

$$\frac{\partial}{\partial t} (\bar{\rho} R_{ij}) + \frac{\partial}{\partial x_m} (\bar{\rho} \tilde{U}_m R_{ij}) = P_{ij} + D_{ij} + \phi_{ij} + \varepsilon_{ij} + V_{ij} \quad (8)$$

where the symbols  $P_{ij}$ ,  $D_{ij}$ ,  $\phi_{ij}$ ,  $\varepsilon_{ij}$  and  $V_{ij}$  represent turbulent production, turbulent diffusion, pressure strain correlation, turbulent dissipation and the mass flux variation respectively.

$$P_{ij} = -\bar{\rho} R_{jm} \tilde{U}_{i,m} - \bar{\rho} R_{im} \tilde{U}_{j,m}, \quad D_{ij} = -(\overline{\rho u_i'' u_j'' u_m''} + \overline{p' u_j''} \delta_{im} + \overline{p' u_i''} \delta_{jm} - \overline{\tau_{im}'' u_j''} - \overline{\tau_{jm}'' u_i''})_{,m},$$

$$\phi_{ij} = \overline{p' (u_{i,j}'' + u_{j,i}'')} = \phi_{ij}^* + 2/3 \overline{p' u_{k,k}''} \delta_{ij}, \quad \varepsilon_{ij} = \overline{\tau_{im}'' u_{j,m}''} - \overline{\tau_{jm}'' u_{i,m}''},$$

$$V_{ij} = -\bar{p}_{,j} \bar{u}_i'' + -\bar{p}_{,i} \bar{u}_j'' + \bar{\tau}_{im,m} \bar{u}_j'' + \bar{\tau}_{jm,m} \bar{u}_i''.$$

The turbulent dissipation in compressible turbulence was proposed by Sarkar[6,13] as

$$\varepsilon = \varepsilon_s + \varepsilon_c \quad (9)$$

where, for homogeneous shear flow turbulence  $\bar{\rho} \varepsilon_s = \overline{\mu \omega_i' \omega_i'}$ ,  $\omega_i'$  is the fluctuating vorticity, and  $\varepsilon_c = 4/3 \overline{\mu u_{k,k}''^2}$  are the incompressible and dilatational or (compressible) parts of the turbulent dissipation rate. The authors argued that the incompressible part of the dissipation can be modeled by using the incompressible equation model, namely

$$\frac{\partial}{\partial t} (\bar{\rho} \varepsilon_s) + \frac{\partial}{\partial x_k} (\bar{\rho} \varepsilon_s \tilde{U}_k) = \bar{\rho} \frac{\varepsilon_s}{K} (C_{\varepsilon 1} R_{km} \frac{\partial}{\partial x_m} \tilde{U}_k - C_{\varepsilon 2} \varepsilon_s) - \frac{\partial}{\partial x_k} (C_{\varepsilon 3} \bar{\rho} \frac{K}{\varepsilon_s} R_{kn} \frac{\partial}{\partial x_m} \varepsilon_s) \quad (10)$$

### 3. Compressible turbulence model for the pressure strain

Many DNS and experiment results have been carried out on compressible turbulent flows, most of which show the significant compressibility effects on the pressure-strain correlation via the pressure fields. Such effects induce reduction in the magnitude of the anisotropy of the Reynolds shear stress and increase in the magnitude of the normal stress anisotropy. Consequently, the pressure strain correlation requires a careful modeling in the Reynolds stress turbulence model. With respect to the incompressible case, many compressible models have been developed for the pressure-strain correlation. Hereafter, most of all these models are generated from a simple extension of its incompressible counter-part as in [13,14,15,16], in general, they perform well in the simulation of important turbulent flows evolving with moderate compressibility.

#### 3.1 Model of Adumitroiaie et al. [13]

Adumitroiaie et al. assumed that incompressible modeling approach of the pressure-strain can be used to develop turbulent models taking into account compressibility effects. Considering a non zero divergence for the velocity fluctuations called the compressibility continuity constraint and using different models for the pressure dilatation which is proportional to the trace of the pressure-strain, their model for the pressure strain is written as follows:

$$\begin{aligned} \phi_{ij}^* = & -C_1 \bar{\rho} \varepsilon_s b_{ij} + \left(\frac{4}{5} + \frac{2}{5} d_1\right) \bar{\rho} K (\tilde{S}_{ij} - \frac{1}{3} \tilde{S}_{ll} \delta_{ij}) + 2\bar{\rho} K (1 - C_3 + 2d_2) [b_{ik} \tilde{S}_{jk} + b_{jk} \tilde{S}_{ik} \\ & - \frac{2}{3} b_{ml} \tilde{S}_{ml} \delta_{ij}] - \bar{\rho} K (1 - C_4 - 2d_2) [b_{ik} \tilde{\Omega}_{jk} + b_{jk} \tilde{\Omega}_{ik} - \frac{4}{3} d_2 \tilde{S}_{kk} b_{ij}] \end{aligned} \quad (11)$$

where  $\tilde{S}_{ij} = 0.5(\tilde{U}_{i,j} + \tilde{U}_{j,i})$ ,  $\tilde{\Omega}_{ij} = 0.5(\tilde{U}_{i,j} - \tilde{U}_{j,i})$  and  $b_{ij} = R_{ij} / 2K - \frac{1}{3} \delta_{ij}$ .

The compressible coefficients  $d_1$  and  $d_2$  are determined from some compressible closures for the pressure-dilatation correlation (see Adumitroiaie et al.[13]).

#### 3.2 Model of Hung et al.[14]

The authors introduces a compressible dumping function of turbulent Mach number to modify the incompressible model of the pressure strain correlation, the model reads :

$$\begin{aligned} \phi_{ij}^* = & -C_1 \bar{\rho} \varepsilon_s b_{ij} + C_2 \bar{\rho} K (\tilde{S}_{ij} - \frac{1}{3} \tilde{S}_{ll} \delta_{ij}) + C_3 \bar{\rho} K [b_{ik} \tilde{S}_{jk} + b_{jk} \tilde{S}_{ik} - \frac{2}{3} b_{ml} \tilde{S}_{ml} \delta_{ij}] \\ & + C_4 \bar{\rho} K [b_{ik} \tilde{\Omega}_{jk} + b_{jk} \tilde{\Omega}_{ik}] \end{aligned} \quad (12)$$

Where  $C_1 = 3.6$ ,  $C_2 = 0.8$ ,  $C_3 = 1.2 + f(M_t)$ ,  $C_4 = 1.2 - f(M_t)$ .

and  $f(M_t) = 0.25 \exp(-0.05 / M_t^3)$

### 4. Compressibility corrections of the SSG and FLT models

In this section, we consider compressibility extensions of two existing incompressible models : Speziale Sarkar and Gatski [11] model and FLT[12] model. The reason behind the choice is the high performance level of these models in simulating variety complex flows. The models are presented in the following forms :

#### 4.1 Speciale Sarkar and Gatski, SSG model [11]

$$\begin{aligned}\phi_{ij}^* = & -(C_1 \bar{\rho} \varepsilon_s + C_1^* \bar{\rho} P) b_{ij} + (C_3 - C_3^* II^{1/2}) \bar{\rho} K (\tilde{S}_{ij} - \frac{1}{3} \tilde{S}_{ll} \delta_{ij}) + \\ & C_2 \bar{\rho} \varepsilon_s (b_{ik} b_{kj} - \frac{1}{3} b_{mk} b_{km} \delta_{ij}) + \bar{\rho} K C_4 [b_{ik} \tilde{S}_{jk} + b_{jk} \tilde{S}_{ik} - \frac{2}{3} b_{ml} \tilde{S}_{ml} \delta_{ij}] + \\ & \bar{\rho} K C_5 [b_{ik} \tilde{\Omega}_{jk} + b_{jk} \tilde{\Omega}_{ik} - \frac{4}{3} d_2 \tilde{S}_{kk} b_{ij}]\end{aligned}\quad (13)$$

where  $C_1, C_1^*, C_2, C_3, C_3^*, C_4$  and  $C_5$  are:  $C_1 = 3.4, C_1^* = 1.8, C_2 = 4.2, C_3 = 0.8, C_3^* = 1.3,$

$C_4 = 1.25, C_5 = 0.4. II = b_{ij} b_{ij}$  and  $P = -R_{ij} \tilde{U}_{i,j}$ .

#### 4.2 Fu, Launder and Tsepidakis, FLT model [12]

$$\begin{aligned}\phi_{ij}^* = & -C_1 \bar{\rho} \varepsilon_s b_{ij} + C_3 \bar{\rho} K (\tilde{S}_{ij} - \frac{1}{3} \tilde{S}_{ll} \delta_{ij}) + C_2 \bar{\rho} \varepsilon_s (b_{ik} b_{kj} - \frac{1}{3} II \delta_{ij}) + \\ & \bar{\rho} K C_4 [b_{ik} \tilde{S}_{jk} + b_{jk} \tilde{S}_{ik} - \frac{2}{3} b_{ml} \tilde{S}_{ml} \delta_{ij}] + \bar{\rho} K C_5 [b_{ik} \tilde{\Omega}_{jk} + b_{jk} \tilde{\Omega}_{ik}] + \\ & \frac{4}{5} \bar{\rho} K [b_{ik} b_{km} \tilde{S}_{jm} + b_{jk} b_{km} \tilde{S}_{im} - 2b_{ik} b_{km} \tilde{S}_{jm} - 3b_{km} b_{ij} \tilde{S}_{km}] - \frac{14}{5} \bar{\rho} K \\ & [8II (b_{ik} \tilde{\Omega}_{jk} + b_{jk} \tilde{\Omega}_{ik}) + 12(b_{ik} b_{kl} b_{mj} \tilde{\Omega}_{lm} + b_{jk} b_{kl} b_{mi} \tilde{\Omega}_{lm}) + \\ & \frac{4}{5} \bar{\rho} K [b_{ik} b_{km} \tilde{\Omega}_{jm} + b_{jk} b_{km} \tilde{\Omega}_{im}]\end{aligned}\quad (14)$$

The coefficients model:  $C_1, C_2, C_3, C_4$  and  $C_5$  are as follows :

$$C_1 = -120II \sqrt{F} - 2\sqrt{F} + 2, C_2 = 144II \sqrt{F}, F = 1 + 9II + 27III, III = \frac{1}{3} b_{ij} b_{kj} b_{ki}$$

$$C_3 = 4/5, C_4 = 6/5, C_5 = 26/5.$$

Theses models can be written in the following unified form :

$$(\phi_{ij}^*) = (\phi_{ij}^*)_1 + (\phi_{ij}^*)_2 \quad (15)$$

Where  $(\phi_{ij}^*)_1$  is linear in terms of the mean strain and Reynolds stress, use formulation similar to it's given by LRR [17].

$$\begin{aligned}(\phi_{ij}^*)_1 = & -\alpha_1 \bar{\rho} \varepsilon_s b_{ij} + \alpha_2 \bar{\rho} K (\tilde{S}_{ij} - \frac{1}{3} \tilde{S}_{ll} \delta_{ij}) + \alpha_3 \bar{\rho} K [b_{ik} \tilde{S}_{jk} + b_{jk} \tilde{S}_{ik} - \frac{2}{3} b_{ml} \tilde{S}_{ml} \delta_{ij}] \\ & + \alpha_4 \bar{\rho} K [b_{ik} \tilde{\Omega}_{jk} + b_{jk} \tilde{\Omega}_{ik}]\end{aligned}\quad (16)$$

whereas the non-linear part  $(\phi_{ij}^*)_2$  is explicitly quadratic in the Reynolds stress and the gradient of velocity. Thus, for the two models [11,12], we can write :

$$\begin{aligned}
(\phi_{ij}^*)_2 = & -\beta_1 \bar{\rho} P b_{ij} + \beta_2 \bar{\rho} \varepsilon_s (b_{ik} b_{kj} - \frac{1}{3} b_{mk} b_{km} \delta_{ij}) + \beta_3 \bar{\rho} K [b_{ik} b_{km} \tilde{S}_{jm} + b_{jk} b_{km} \tilde{S}_{im} - 2b_{ik} b_{jm} \tilde{S}_{km} \\
& - 3b_{ij} b_{km} \tilde{S}_{km}] - \beta_4 [b_{ik} b_{km} \tilde{\Omega}_{jm} + b_{jk} b_{km} \tilde{\Omega}_{im}] + \beta_5 \bar{\rho} K [b_{ik} b_{kl} b_{mj} \tilde{\Omega}_{lm} + b_{jk} b_{kl} b_{mi} \tilde{\Omega}_{lm}]
\end{aligned} \quad (17)$$

All correspondent coefficients model are summarized in Table1.

Because the incompressible LRR model is successfully extended to different complex turbulent compressible flows and because the term  $(\phi_{ij}^*)_1$  is formally identical to the LRR model[17] but the coefficients models are different. Here, we concentrate our attention on the modification of  $(\phi_{ij}^*)_1$  and we propose to write :

$$(\phi_{ij}^*)^{comp} = (\phi_{ij}^*)_1^{comp} + (\phi_{ij}^*)_2 \quad (18)$$

**Table 1 coefficients models**

Model	$\alpha_1$	$\alpha_2$	$\alpha_3$	$\alpha_4$	$\beta_1$	$\beta_2$	$\beta_3$	$\beta_4$	$\beta_5$
LRR	3	0.8	1.75	1.31	0	0	0	0	0
SSG	3.4	$0.8 - 1.3II^{0.5}$	1.25	0.4	-1.8	4.2	0	0	0
FLT	$-120II\sqrt{F} - 2\sqrt{F} + 2$	0.8	$\frac{6}{5} - \frac{122}{5}II$	$\frac{26}{15}$	0	$144II\sqrt{F}$	0.8	0.8	$-\frac{168}{5}II$

Different compressible models can be used for  $(\phi_{ij}^*)_1^{comp}$ , which are essentially extension of the LRR model [17] using different extra compressibility parameters like pressure variance, gradient Mach number and turbulent Mach number. Two compressible models due to Adumitroaie et al.[13] and Hung et al. [14] are used to express  $(\phi_{ij}^*)_1^{comp}$ . Thus, the SSG and FLT models [11, 12] become dependent on the turbulent Mach turbulent number :

$$(\phi_{ij}^*) = ((\phi_{ij}^*)_1^{comp})^{Adumitroaie} + (\phi_{ij}^*)_2 \quad (19)$$

and

$$(\phi_{ij}^*) = ((\phi_{ij}^*)_1^{comp})^{Hung} + (\phi_{ij}^*)_2 \quad (20)$$

All the model constants are summarized in Table 1.

Regarding the models of Adumitroaie et al.[13] and Hung et al.[14], all modified models

numerical coefficients as SSG and FLT models are summarized in Table.2.

**Table 2 Coefficients models**

Model	$\alpha_1$	$\alpha_2$	$\alpha_3$	$\alpha_4$
SSGA	3.4	0.8	$1.25 + f(M_t)$	$0.4 - f(M_t)$
SSGH	3.4	0.8	$1.25 + g(M_t)$	$0.4 - g(M_t)$
FLTA	$-120H\sqrt{F} - 2\sqrt{F} + 2$	0.8	$6/5 - 122H/5 + f(M_t)$	$26/15 + f(M_t)$
FLTH	$-120H\sqrt{F} - 2\sqrt{F} + 2$	0.8	$6/5 - 122H/5 + g(M_t)$	$26/15 + g(M_t)$

Where  $f(M_t) = 0.3M_t^2$  and  $g(M_t) = 0.25 \exp(-0.05/M_t^3)$ .

The SSGA, SSGH, FLTA and FLTH are the proposed compressibility corrections of the incompressible models SSG and FLT by using the compressible models of Adumitroaie et al.[13] and Hung et al.[14] respectively.

## 5. Applications of the models

### 5.1 Simulation of compressible homogeneous shear flow

For compressible homogeneous shear flow, the mean velocity gradient is given by :

$$\tilde{U}_{i,j} = S\delta_{i1}\delta_{j2} \quad (21)$$

where  $S$  is the mean shear rate.

The Favre averaged basic second order model equations are:

$$\bar{\rho} \frac{d}{dt} (R_{ij}) = P_{ij} + \phi_{ij}^* - \frac{2}{3} \bar{\rho} (\varepsilon_s + \varepsilon_c) \delta_{ij} + \frac{2}{3} \overline{p'd'} \delta_{ij} \quad (22)$$

$$\bar{\rho} \frac{d}{dt} \varepsilon_s = C_{\varepsilon 1} \bar{\rho} \frac{\varepsilon_s}{K} R_{km} \frac{\partial}{\partial x_m} \tilde{U}_k - C_{\varepsilon 2} \bar{\rho} \frac{\varepsilon_s^2}{K} \quad (23)$$

The turbulent Mach number is described by the transport equation as follow [20]

$$\frac{d}{dt} M_t = \frac{M_t}{2\bar{\rho}K} (1 + 0.5\gamma(\gamma-1)M_t^2) (\overline{p'd'} - \bar{\rho}\varepsilon) + \frac{M_t}{2K} P \quad (24)$$

where  $P = -\bar{\rho}R_{ij}\tilde{U}_{i,j}$  is the turbulent production and  $\gamma = \frac{c_p}{c_v}$ .

## 5.2 Simulation of compressible mixing layer

The flow is governed by the averaged Navier-Stokes equations associated to those describe the energy, the Reynolds stress and the turbulent dissipation. The simplest of resulting continuity, momentum and energy equation for stationary mixing layers can be written as in[16]:

$$\frac{\partial}{\partial x_i} \bar{\rho} \tilde{U}_i = 0 \quad (25)$$

$$\frac{\partial}{\partial x_i} (\bar{\rho} \tilde{U}_i \tilde{U}_j) = - \frac{\partial}{\partial x_j} (\overline{\rho u_i'' u_j''}) \quad (26)$$

$$\frac{\partial}{\partial x_j} (\bar{\rho} C_v \tilde{T} \tilde{U}_j) = - \frac{\partial}{\partial x_j} (C_v \overline{\rho u_j'' T''}) + \varepsilon_s + \varepsilon_c - \overline{p' u_{i,i}'} \quad (27)$$

The Reynolds stress are solutions of the follow equation

$$\frac{\partial}{\partial x_m} (\bar{\rho} \tilde{U}_m R_{ij}) = -(R_{im} \tilde{U}_{j,m} + R_{jm} \tilde{U}_{i,m}) + \frac{\partial}{\partial x_m} (\overline{\rho u_i'' u_j'' u_m''}) + \phi_{ij}^* + \frac{2}{3} \overline{p' u_{i,i}'} \delta_{ij} - \frac{2}{3} \varepsilon \delta_{ij} \quad (28)$$

The turbulent solenoidal dissipation rate shall be calculated from the classical model equation, namely

$$\frac{\partial}{\partial x_k} (\bar{\rho} \varepsilon_s \tilde{U}_k) = \bar{\rho} \frac{\varepsilon_s}{K} (C_{\varepsilon 1} R_{km} \frac{\partial}{\partial x_m} \tilde{U}_k - C_{\varepsilon 2} \varepsilon_s) - \frac{\partial}{\partial x_k} (C_{\varepsilon 3} \bar{\rho} \frac{K}{\varepsilon_s} R_{km} \frac{\partial}{\partial x_m} \varepsilon_s) \quad (29)$$

In the above mentioned transport equations, different terms should be modeled, the gradient diffusion hypothesis is used to represent:

-The turbulent heat flux[10]:

$$\overline{\rho u_i'' T''} = -C_T \frac{K}{\varepsilon} \overline{\rho u_i'' u_m''} \frac{\partial}{\partial x_m} \tilde{T} \quad (30)$$

-The diffusion term[10]

$$\overline{\rho u_i'' u_j'' u_m''} = -C_s \frac{K}{\rho \varepsilon} \overline{\rho u_i'' u_m''} \frac{\partial}{\partial x_m} \overline{\rho u_j'' u_m''} \quad (31)$$

## 6. Results and Discussions

For the turbulent dilatational part of the dissipation and the correlation pressure-dilatation, we chose the models proposed by Sarkar[10,21], namely

$$\varepsilon_d = 0.5 M_t^2 \varepsilon_s \quad (32)$$

$$\overline{p' u_{i,i}'} = 0.15 M_t \bar{\rho} (R_{ij} - \frac{2}{3} K \delta_{ij}) + 0.2 \bar{\rho} M_t^2 \varepsilon_s \quad (33)$$



### 6.1 Homogeneous shear flow

**Table 3 Initial conditions for homogeneous shear flow :DNS[1]**

case	$M_{i0}$	$M_{g0}$	$(SK/\varepsilon_s)_0$	$b_{11}$	$b_{11}$	$b_{12}$
$B_1$	0.25	0.6	8	0	0	0
$B_3$	0.25	1.9	24	0	0	0

**Table 4 Initial conditions for homogeneous shear flow :DNS[6]**

case	$M_{i0}$	$M_{g0}$	$(SK/\varepsilon_s)_0$	$b_{11}$	$b_{11}$	$b_{12}$
$A_1$	0.4	0.22	1.8	0	0	0
$A_4$	0.4	1.32	10.8	0	0	0

The ability of the proposed model for the pressure-strain correlation to predict of the compressible homogeneous turbulent shear flow will now be considered. The above averaged transport equations (22 to 24) are solved numerically for compressible homogeneous turbulence using a fourth-order Runge-Kutta numerical scheme. Figures 1 to 4 show comparison between the predictions obtained by the proposed models referred to SSGA, SSGH, FLTA and FLTH (see Tab.2) and those from the incompressible SSG, FLT models[11,12] and with the DNS results[1,6]. All these cases of DNS correspond to different initial conditions listed in Tables 3 and 4.

From all figures, it is clear that the SSG and FLT incompressible models[11,12] are still unable to predict the dramatic changes in the magnitude of the Reynolds-stress anisotropy that arise from compressibility. All the proposed modifications of the SSG model provide an acceptable performance in reproducing the DNS results for all cases.

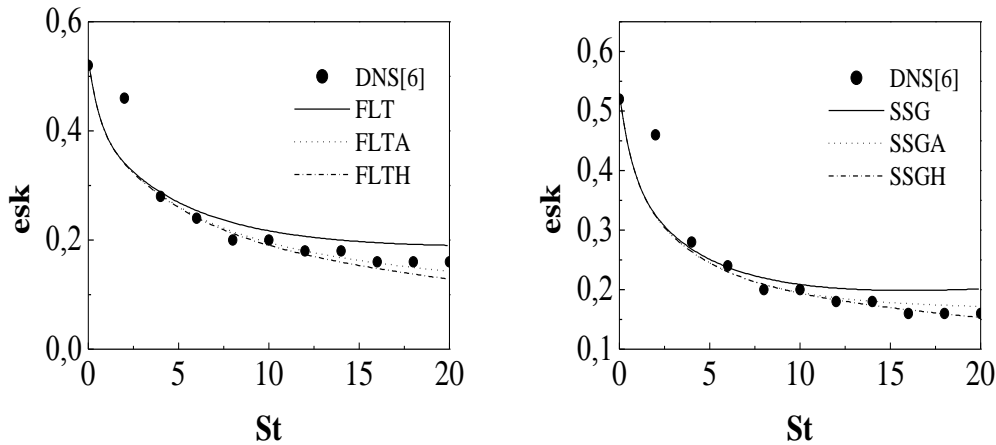


**Fig.1 Time evolution of the normalized dissipation ( $esk = \varepsilon_s / SK$ ) in the case:  $B_1$**

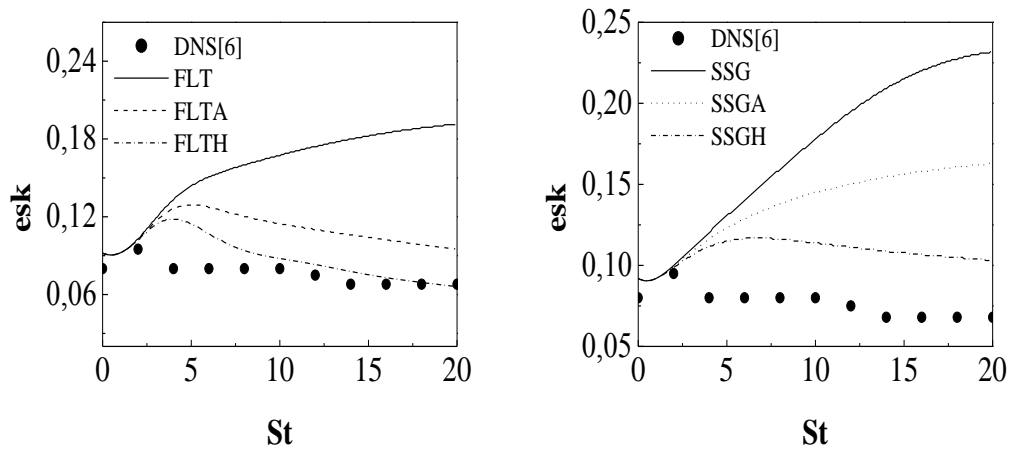


**Fig.2 Time evolution of the normalized dissipation ( $esk = \varepsilon_s / SK$ ) in the case:  $B_3$**

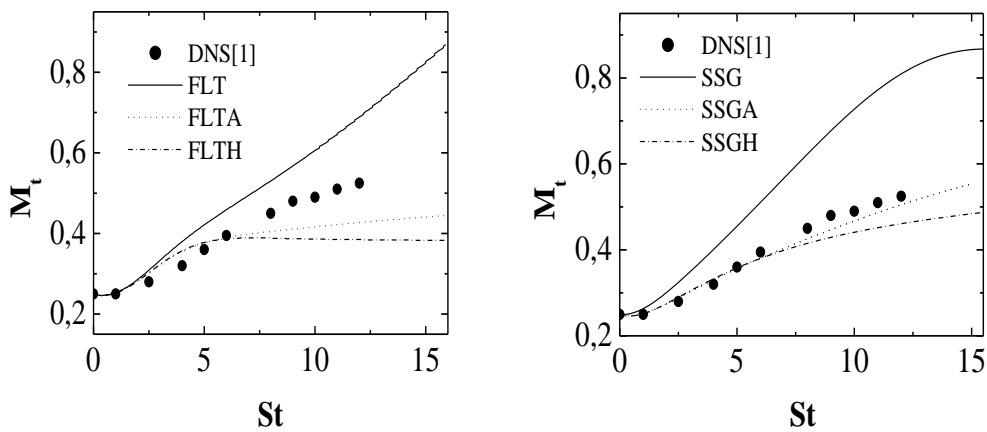


**Fig.3 Time evolution of the turbulent Mach number ( $M_t$ ) in the case:  $B_1$**

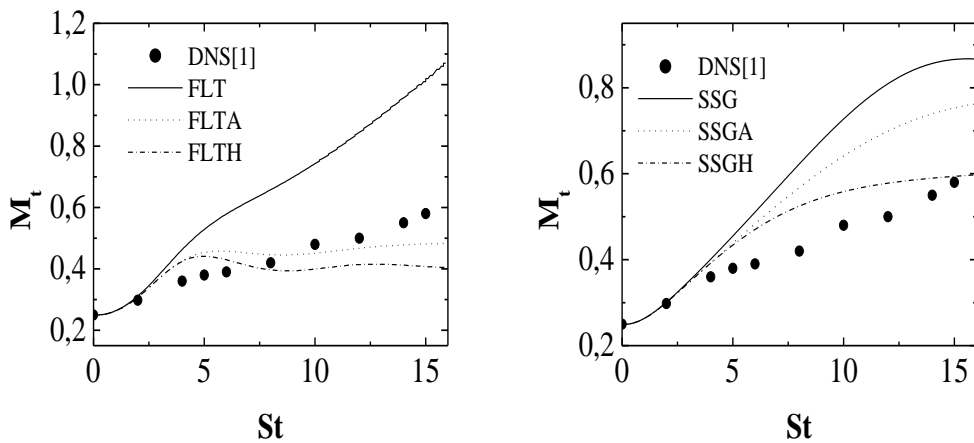
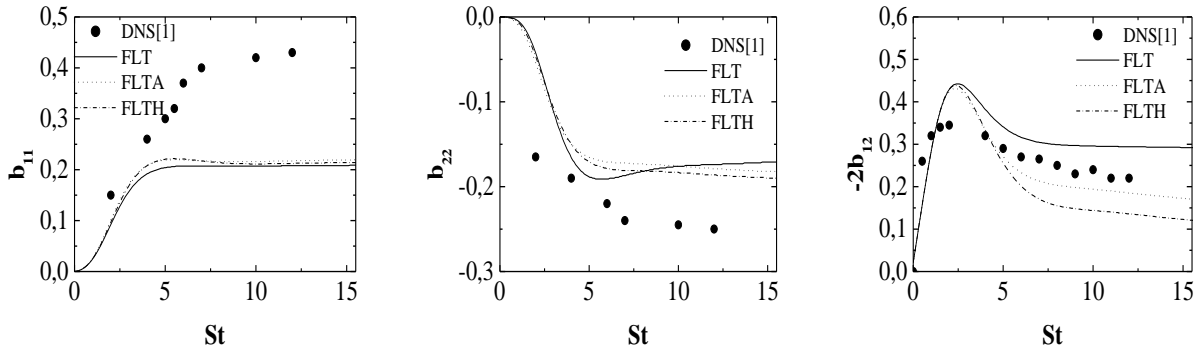


**Fig.4 Time evolution of the turbulent Mach number ( $M_t$ ) in the case:  $B_3$**

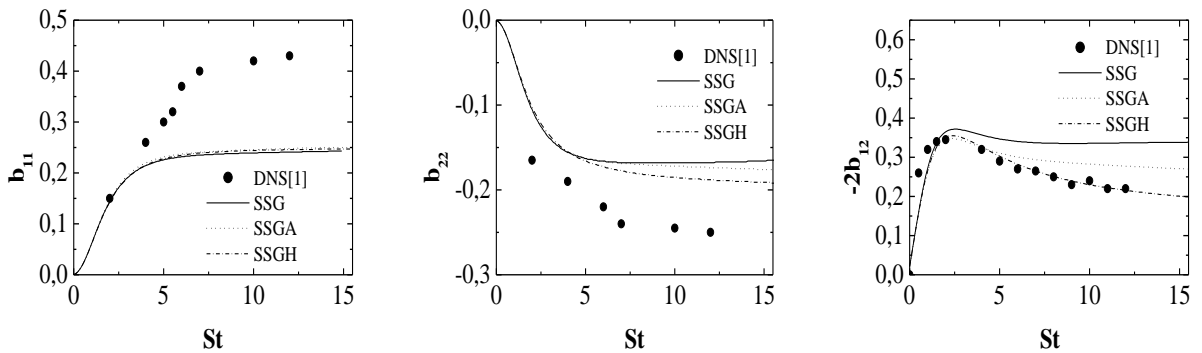
Figures 1 and 2 show the normalized dissipation  $\varepsilon_s / SK$  for cases:  $A_1$  and  $A_4$  from DNS[6]. The proposed compressibility corrections of SSG and FLT models are in acceptable accordance with the DNS results of Sarkar[6]. It is clearly seen that all of the models appear to be able to predict accurately the trend of the decrease of  $\varepsilon_s / SK$  when  $M_{g0}$  increases since the compressibility effects cause significant reduction in the production from numerical simulation cases  $A_1$  to  $A_4$ .

Figure 2 shows the time evolution of the turbulent Mach number. The proposed models yield reasonable acceptable results that are in good qualitative agreement with the DNS results of Simone et al.[1]. The proposed models appear to be able to predict the trend of the  $M_t$ -increase with increasing the initial value of the gradient Mach number.

Figures 5 to 8 show the non-dimensional time (St) variation of the Reynolds stress anisotropies  $b_{11}$ ,  $b_{22}$  and  $b_{12}$ . From these figures, it is clear that the proposed model appears to be able to predict correctly the significant decrease of the normalized turbulent production term with increasing the gradient Mach number. All the models SSGA, SSGH, FLTA and FLTH appear to be insensitive to the increase of the streamwise  $b_{11}$ , the transverse  $b_{22}$  Reynolds stress anisotropies when the compressibility increases. SSG[11] and FLT[12] models results are in disagreement with the DNS data especially at high  $M_g$  in case:  $B_3$ , this model is still unable to predict the changes in the magnitude of the Reynolds stress anisotropy when the compressibility is higher. Figures 9 to 12 present the behavior of the pressure strain correlation  $(P_{ij}) = \phi_{ij}^* / 2SK$ . As can be seen in these figures, the proposed models yield acceptable results that are in good qualitative agreement with the DNS data especially at high gradient Mach number.



**Fig.5 Time evolution of the Reynolds stress anisotropies in the case:  $B_1$ .**



**Fig.6 Time evolution of the Reynolds stress anisotropies in the case:  $B_1$ .**

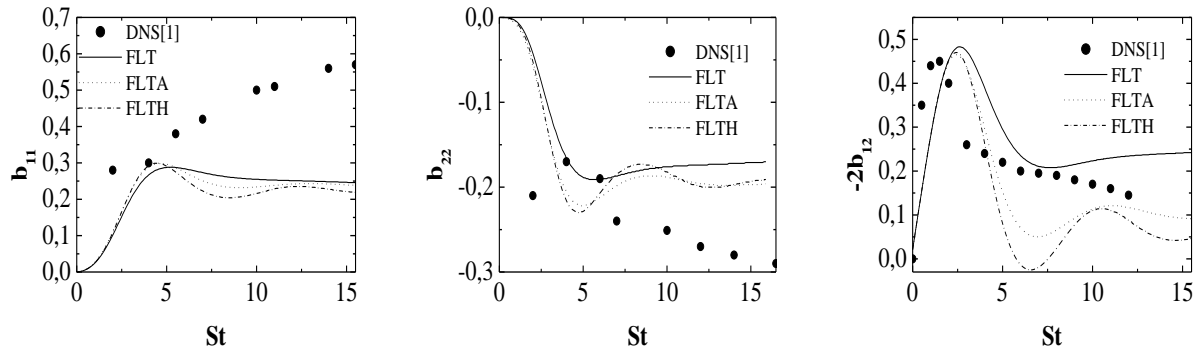


**Fig.7** Time evolution of the Reynolds stress anisotropies in the case:  $B_3$

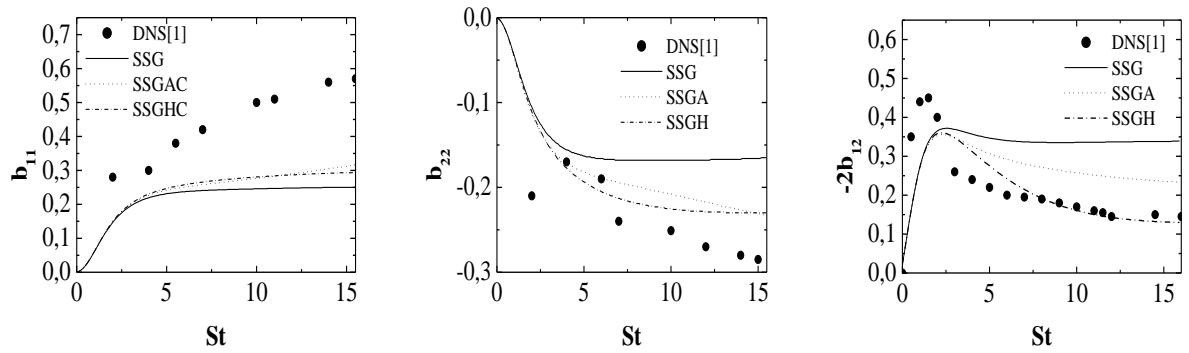


**Fig.8** Time evolution of the Reynolds stress anisotropies in the case:  $B_3$

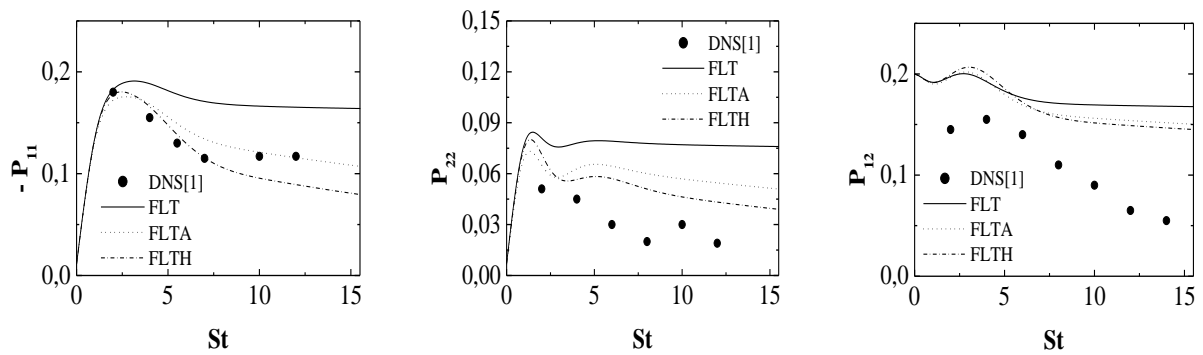


**Fig.9** Time evolution of the pressure strain components in the case:  $B_1$

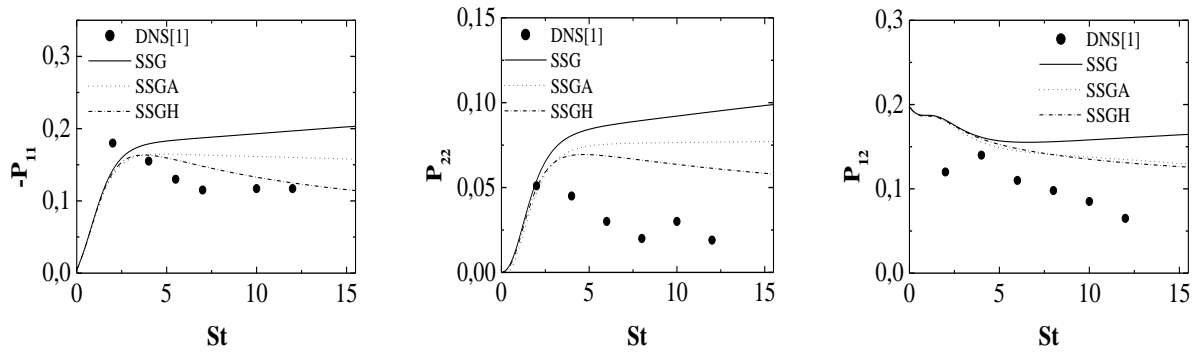


Fig.10 Time evolution of the pressure strain components in the case:  $B_1$ .

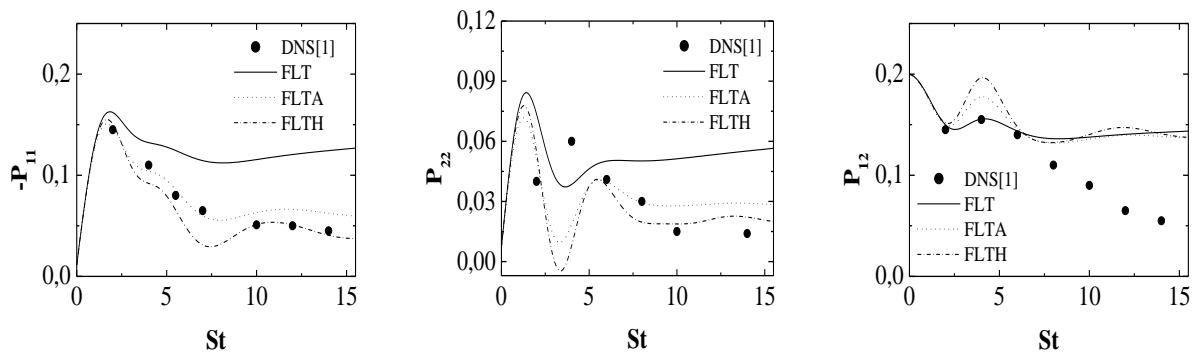


Fig.11 Time evolution of the pressure strain components in the case:  $B_3$ .

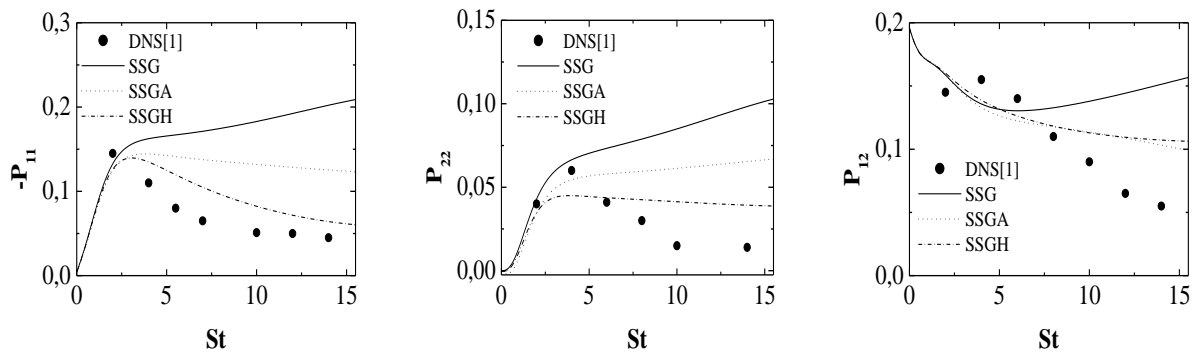
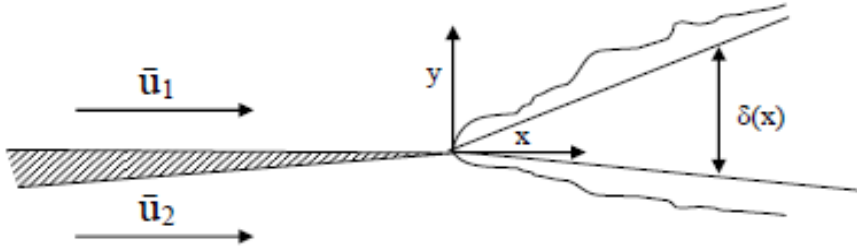


Fig.14 Time evolution of the pressure strain components in the case:  $B_3$ .

From the previous results, one can see that for cases  $B_1[1]$  and  $A_1[6]$  which correspond to low compressibility, all the models : original and modified versions of SSG and FLT models are nearly similar, the difference between their predictions are smaller. These difference become apparent for the majority turbulence characteristic parameters at high compressibility, the initial values of the turbulent Mach gradient are higher as in cases  $B_2[1]$  and  $A_4[6]$ . It is clear that, one can remarks that the proposed models SSGA and SSGH predictions are more better than those obtained by the FLTA and FLTH models. Thus, the compressibility correction of the SSG model of the pressure strain correlation is found out to be an important issue for amelioration of the performance level in prediction of compressibility effects.

## 6.2 Compressible mixing layer

From many several researches concerning mixing layers flows, we argue that the pressure strain correlation is one the mean term contributing to the reduced growth rate and the changes of the Reynolds stress arising from compressibility effects. Modeling turbulent pressure strain correlation occurs mainly at high speed for mixing layers which are known to be influenced by compressibility effects.



**Fig.12 Turbulent mixing layers**

The basic equations 25 to 28 on which the second order model for the stationary compressible mixing layers is based are solved using a finite difference scheme. The grid of computational physical domain which is rectangular box defined by the set of point  $(x, y)$  has 6666x41 points. The initial profiles for  $\varepsilon_s$ ,  $\bar{\rho}$  and  $\tilde{T}$  which are not available in the experience of Goebel and Dutton[7] are generated as: the initial profile of the turbulent dissipation is determined from the turbulent viscosity model.

$$\varepsilon_s = -C_\mu \bar{\rho} \frac{K^2}{\rho u'' v''} \frac{\partial \tilde{U}}{\partial y} \quad C_\mu = 0.09 \quad (34)$$

The initial profile of the temperature is obtained from the following similarity

$$\frac{\tilde{U} - U_2}{\Delta U} = \frac{\tilde{T} - T_2}{\Delta T} \quad (35)$$

The state equation of perfect gas is used to determine the initial profile of the density.

We have calculated two free streams of a fully developed compressible mixing layers (see fig.12) which are characterized typically by the convective Mach number  $M_c$  and the parameters  $s = \rho_2/\rho_1$  and  $r = U_2/U_1$ , are respectively the density and velocity ratios, the experiment conditions of Goebel et al.[7] are listed in tab.5.

**Table 5 Experience of Goebel and Dutton[7]**

$M_c$	0.2	0.46	0.69	0.86	1
$r = \frac{U_2}{U_1}$	0.78	0.57	0.18	0.16	0.16
$s = \frac{\rho_2}{\rho_1}$	0.76	1.55	0.57	0.6	1.14

The values of the constants models used in the present simulation are:

$$C_{\varepsilon_1} = 1,4, C_{\varepsilon_2} = 1,8, C_\mu = 0,09, C_\varepsilon = 0,25, C_T = 0,26.$$

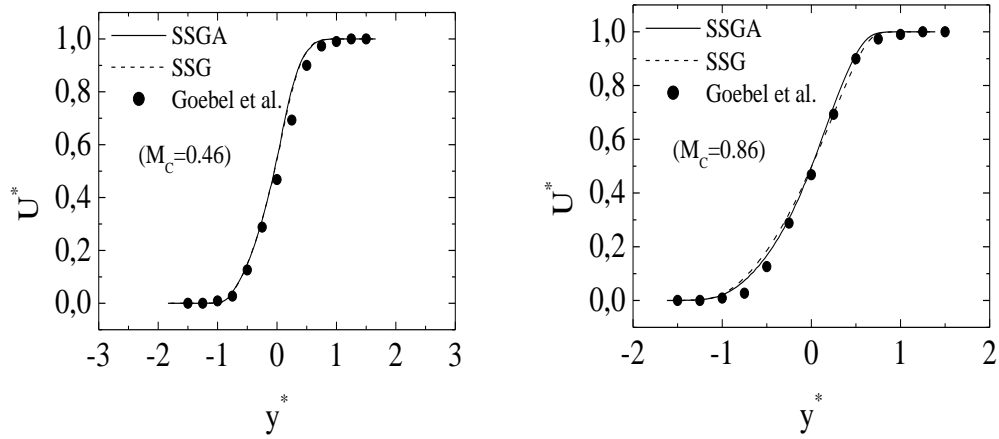


**Fig.13** Similarity profiles of the mean velocity  $U^* = (\tilde{U} - U_2)/(U_1 - U_2)$ .

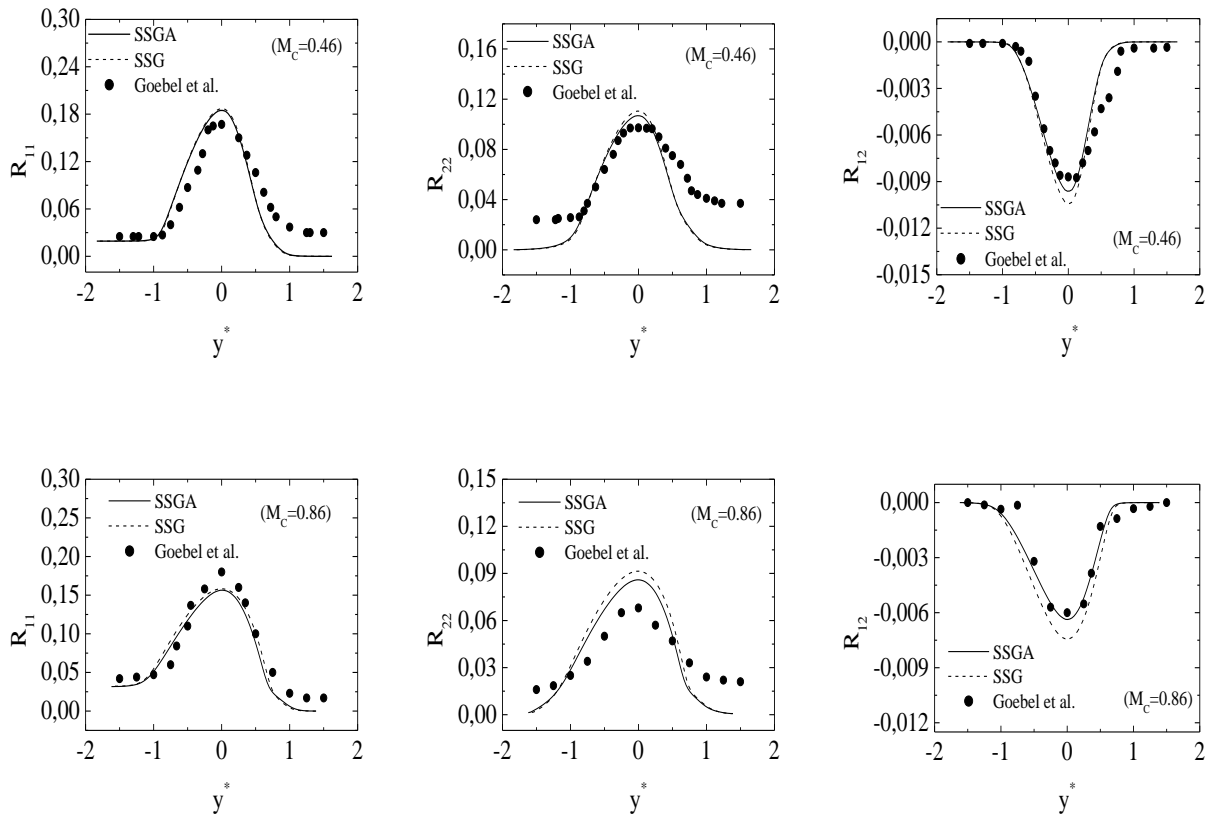


**Fig.14** Similarity profiles of Reynolds intensities

In all sets of experiments, we choose two cases that correspond to  $M_c = 0.46$  and  $M_c = 0.86$ .

The proposed model (SSGA) predictions will be compared with those obtained by the incompressible SSG

model and the experiment results of Goebel et al.[7]. Figure 13 shows the normalized stream mean velocity  $U^* = (\tilde{U} - \tilde{U}_2)/(\tilde{U}_1 - \tilde{U}_2)$  in relation to the similarity variable  $y^* = (y - y_c)/\delta$ , where  $y$  is the local cross stream coordinate and  $y_c$  is the cross-stream coordinates corresponding to  $U^* = 0.5$ . The calculated velocity profiles by the two models SSG and SSGA are in reasonable agreement with experimental results[7]. Figures 14 shows the effects of compressibility of the changes in the Reynolds stress : the streamwise turbulence intensity  $R_{11} = \sqrt{\overline{\rho u''^2} / \bar{\rho}(U_1 - U_2)^2}$ , the transverse turbulence intensity  $R_{22} = \sqrt{\overline{\rho v''^2} / \bar{\rho}(U_1 - U_2)^2}$  and the shear stress  $R_{12} = \overline{\rho u''v''} / \bar{\rho}(U_1 - U_2)^2$ . Examination of these figures indicates that the proposed model predictions of these turbulent quantities are in good agreement with the experimental results[7] for the two values of the convective Mach number. One can see the decrease of the transverse component and the shear stress  $(R_{22})_{\max}$  computed values by the proposal model as the convective Mach number increases, the values are in accordance with the experimental results[7]. The proposed model computed  $(R_{11})_{\max}$  values of the streamwise normal stress are not affected by the variation of the convective Mach number as shown in previous experiments[7]. The universally SSG model predictions of these quantities are in disagreement with the experimental data[7] especially in high compressibility  $M_c = 0.86$ . The SSG model underestimates  $(R_{11})_{\max}$  and over predicts  $(R_{22})_{\max}$  and  $(R_{12})_{\max}$ .

## 7. Conclusion

In this study, an evaluation of the turbulence models for prediction of compressible turbulent flows is made with using the second order closure. The standard Reynolds-stress turbulence model with the addition of the pressure-dilatation and compressible dissipation models yields the same results as in the incompressible case, it gives very poor predictions of the changes in the Reynolds-stress anisotropy magnitude. The deficiency of this closure is due to the use of the incompressible models of the pressure-strain correlation. A compressibility corrections of the SSG model[11] and FLT [12] model have been proposed to reflect compressibility effects. Application of the models to predict two turbulent compressible flows: homogeneous shear flow and mixing layers shows satisfactory agreement with available DNS[1,6] and experimental results[7]. These proposed models appear to be able to predict accurately the structural compressibility effects on homogeneous shear flow as the significant decrease in the magnitude of the Reynolds shear stress and the reduction of the pressures strain components with increasing initial values of the gradient Mach number. Also, The present models, successfully predict the changes in the similarity of the Reynolds intensities arising from compressibility effects on the mixing layers. Therefore, a priori, the extension of the incompressible non linear SSG and FLT models by using the turbulent Mach number is found out to be important issue in the modeling of the pressure-strain correlation with respect to compressible turbulent flows.

## References

- [1] Simone,S.,Coleman,G.N and Cambon,C., The effect of compressibility on turbulent shear flow: a



- rapid distortion-theory and direct numerical simulation study, *J.Fluid Mech.*330(1997),pp.307-338.
- [2] ggarwal, A. K., Verma, A.: The Effect of Compressibility, Rotation and Magnetic field on thermal instability of walters' fluid permeated with suspended particles in porous medium, *Thermal Sciences* 2014, Vol. 18, Suppl. 2, pp. S539-S550
- [3 ] Fujihiro,H.,Effets of pressure fluctuations on turbulence growth compressible homogeneous shear flow,*Phys.Fluid*,A6(1999),1625.
- [4] Vreman,A.W.,Sandham, N.D and Luo,K.H.,Compressible mixing layer growth rate and turbulence characteristics, *J.Fluid Mech.*,330(1996),pp.235-258.
- [5] Pantano, C., Sarkar, S., A study of compressibility effects in the high speed turbulent shear layer using direct simulation, *J. Fluid Mech.*, 451 (2002), pp. 329-371.
- [6] Sarkar, S. , The stabilizing effects of compressibility in turbulent shear flows, *Journal of Fluid Mech.* 282(1995), pp.163-186.
- [7] Goebel S.G, Dutton J.C., Experimental study of compressible mixing layers, *AIAA Journal*,29 (1991), pp. 538-546.
- [8] Samimy M, Elliot G.S., Effects of compressibility on the characteristics of the free shear layers, *AIAA Journal*.89(1990),pp.439-445.
- [9] Blaisdell, G.A. and Sarkar, S., Investigation of the pressure-strain correlation in compressible homogeneous turbulent shear flow, *ASME FED*,151(1993), pp.133-138.
- [10] Speziale C.G, Sarkar S.,Second order closure models for supersonic turbulent flows, *NASA Langley Research center ,Hampton,ICASE Report*(1991).
- [11] Speziale C.G, Sarkar S.,Gatski T.B.,Modelling the pressure strain correlation of turbulence an invariant dynamical systems approach, *J.Fluid Mech.*,227(1990),pp.245.
- [12] Launder B E., Fu S., Tselepidakis S., Accomodating the effets of hig strain rates in modeling the pressure strain correlation TFD/5(1987).
- [13] Adumitroiae V., Ristorcelli J.R and Taulbee D.B. ,Progress in Favre Reynolds stress closures for compressible flows, *Phys.Fluids*,A11(1999),pp.2696-2719.
- [14] Hung S,Song Fu., Modelling of pressure strain correlation compressible turbulent flow., *Acta Mech Sin*24(2008),pp37-43.
- [15] Hamed,M.,Hechmi,K.,Taieb,L.,Extension of the Launder Reece and Rodi on compressible Homogeneous shear flow, *Eur.Phys. J.B*,45(2005),pp.147-154.
- [16] Hechmi,K., Taieb,L.,On the compressibility effects in mixing layers.,*Thermal Sciences* 2014,pp.59.
- [17] Launder B.E., Reece G.J and Rodi, Progress in the development of a Reynolds-stress turbulence closure, *J.Fluid Mech.*,68(1975), pp.537-566.